IJMOT

INTERNATIONAL JOURNAL OF MICROWAVE AND OPTICAL TECHNOLOGY,

VOL.4 NO.6 NOVEMBER 2009

A Rigorous Study of Some Planar Structures With Longitudinally Magnetized Ferrite by a Modified LSBR Method

Hedi SAKLI2(*), Hafedh BENZINA[1], Taoufik AGUILI[2], Jun. Wu. TAO[3]

[1]Ecole Nationale d'Ingénieurs de Gabès, Rue Omar Ibn El Khattab, 6029 Gabès, Tunisia
e-mail : hafed.benzina@ieee.org
[2]Ecole Nationale d'Ingénieurs de Tunis (Labo SYS'COM), B.P :37, Le Belvédère, 1002 Tunis, Tunisia
*e-mail : **saklihedi@yahoo.fr** ; tél : (00216)97 904 982
e-mail : taoufik.aguili@enit.enu.tn
[3]Groupe de Recherche en Electromagnétisme (GRE), ENSEEIHT-INPT, 31071 Toulouse, France
e-mail : tao@enseeiht.fr

***Abstract*- In this paper, we propose a variant of the least squares boundary residual (LSBR) method which takes into account the singularities of the electromagnetic field in the metal-dielectric edge due to the existence of the Gibbs phenomenon. A Systematic weight functions are employed in this method permitting to obtain accurate and efficient numerical results with an accelerated convergence. We present the extension of the modified LSBR method to the study of the dispersion of the planar structures partially full of ferrite longitudinally magnetized by a static magnetic field $\overrightarrow{H}_0$, containing conductors of negligible thickness in the interfaces. We modelise the strutures of the microstrip and finlines by a proposed general configuration.**

***Keywords*- anisotropic, dispersion, ferrites, modified LSBR method, planar lines.**

I. INTRODUCTION

Recently, the electromagnetic modeling of microwaves planar structures has been an attractive subject of research due to its use in high frequencies and complex configurations. The conception of these structures requires a rigorous characterization of their performances. Various techniques have been then applied.

Among these, the LSBR method has been applied with success to dispersion problems of the electromagnetic waveguides [1], because it permits to analyse structures with arbitrary geometry and edge problem. It is particularly interesting due to its systematic advantage of not presenting wrong solutions which can happen with the Galerkin method [2,3]. Other techniques of electromagnetic modelling like the approach of the spectral domain (SDA), are affected by the convergence problem [3,4] due to the singularity of the field in the metal-dielectric edge. Compared with other analytical techniques, the LSBR method is a process rigorously convergent without being affected by this phenomenon. There is another recent technique which uses the planar structure analysis with ferrite such the one in [5] where the coupled mode approach is applied to the ferrite circular waveguide magnetized through a rotary four-pole transverse bias magnetic fields. Another study using this technique is also presented in [6] using an extension of the coupled-mode theory for microstrip lines on an isotropic substrate.

In the reference [1], the LSBR method was applied for isotropic planar structures without considering the field singularities to the metal-dielectric discontinuities. The reference [7] presents an analysis of inhomogeneous and isotropic structures with the consideration of the Gibbs phenomenon caused by those singularities. And that is called the modified LSBR (or LSBRM). We propose a rigorous study of the anisotropic and inhomogeneous planar structures.

We compare the two methods: LSBR and LSBRM, and we make an extension of this analysis for the case of ferrites.

Our study is essentially dedicated to determine the propagation constant k_z in this kind of planar structures. The obtained results of the propagation constant form a perfect match with those published in the literature.

II. THEORY

At the microwaves frequencies, the ferrites are characterized by a tensorial permeability which represents their induced anisotropy under a magnetic field. The permeability of longitudinally magnetized ferrite is described by the Polder tensor

$$\overline{\overline{\mu}} = \mu_0 . \begin{bmatrix} \mu & -j\kappa & 0 \\ j\kappa & \mu & 0 \\ 0 & 0 & \mu_{rz} \end{bmatrix} = \mu_0 . \overline{\overline{\mu}}_{rf} \qquad (1)$$

Where μ, κ and μ_{rz} are real quantities.

For a partial magnetization of the ferrite, Green [8] and Schloemann [9] give the empirical expressions of μ, κ and μ_{rz}

$$\mu_d = \frac{1}{3}\left[1+2\sqrt{1-\left(\frac{\omega_m}{\omega}\right)^2}\right] \qquad (2)$$

Where $\omega_m = \gamma(4\pi M_s)$, ω is the pulsation, γ is the gyromagnetic constant $(\gamma = 2.8\ MHz/Oe)$, $4\pi M_s$ is the saturation magnetization and $4\pi M$ is the magnetization.

$$\mu = \mu_d + (1-\mu_d)\left(\frac{4\pi M}{4\pi M_S}\right)^{3/2} \qquad (3)$$

$$\kappa = \frac{\gamma(4\pi M)}{\omega} \qquad (4)$$

$$\mu_{rz} = \mu_d . {}^{1-\left(\frac{4\pi . M}{4\pi . M_S}\right)^{5/2}} \qquad (5)$$

The general structure is a rectangular waveguide, formed by many layers of dielectrics (isotropic) and one or many layers of longitudinally magnetized ferrite (anisotropic), homogenous in the direction-oy (Fig. 1).

The interface Ω_i, between the two regions (i) and $(i+1)$ can contain metal of negligible thickness and infinite conductivities. We notice, then $\Omega_i = \Omega_i^{(I)} \cup \Omega_i^{(M)}$. Where $\Omega_i^{(I)}$, $\Omega_i^{(M)}$ are respectively the dielectric domain and the metal surface in the interface level Ω_i.

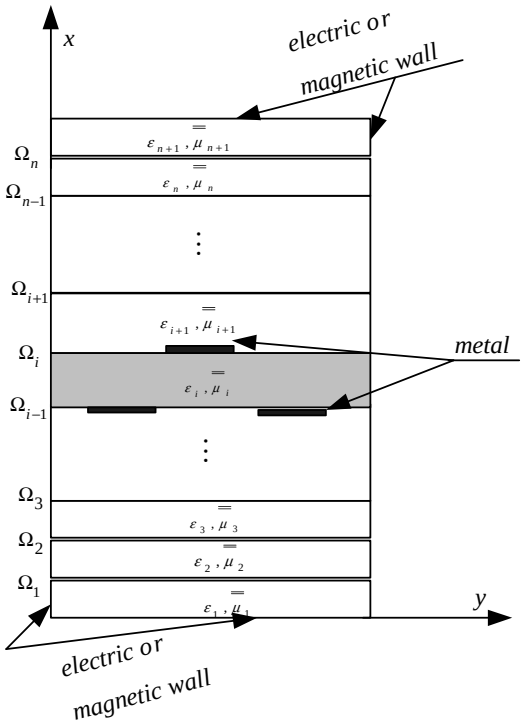

Fig.1. A cross section of the waveguide

The electric field in different mediums is given by

$$E^{(i)}(x,y,z) = E^{(i)}(x,y).e^{j(\omega.t-k_z.z)} \qquad (6)$$

In the following, we will omit the temporal dependency to simplify the notations $e^{j\omega t}$.

Due to the non-homogeneity in the direction-ox, it is preferred to develop the electromagnetic field in different regions by the superposition of modes TE and TM (or LSE and LSM). The presence of the metal in the interfaces will couple these two types of modes to give hybrid modes LSE and LSM, for a given region, from the potentials of Hertz Π_e electric and Π_h magnetic.

$$E_i = -j\omega\overline{\overline{\mu}}_i \nabla\times\Pi_h + \nabla\times\nabla\times\Pi_e \qquad (7a)$$

$$H_i = \nabla\times\nabla\times\Pi_h + j\omega\varepsilon_i \nabla\times\Pi_e \qquad (7b)$$

Where : i region index; $\varepsilon_i = \varepsilon_0\varepsilon_{ri}$; $\overline{\overline{\mu}}_i = \mu_0\overline{\overline{\mu}}_{ri}$

For a medium longitudinally magnetized ferrite, the components of the tangential electromagnetic field in the plan of discontinuity are given by

$$\begin{bmatrix} E_y \\ E_z \end{bmatrix} = \begin{bmatrix} \dfrac{\partial^2}{\partial x\partial y} & -j\omega\mu_0\mu\dfrac{\partial}{\partial z} \\ \dfrac{\partial^2}{\partial x\partial z} & j\omega\mu_0\mu_{rz}\dfrac{\partial}{\partial y} \end{bmatrix} \begin{bmatrix} \Pi_e \\ \Pi_h \end{bmatrix} \qquad (8a)$$

$$\begin{bmatrix} H_y \\ H_z \end{bmatrix} = \begin{bmatrix} j\omega\varepsilon_i\dfrac{\partial}{\partial z} & \dfrac{\partial^2}{\partial x\partial y} \\ -j\omega\varepsilon_i\dfrac{\partial}{\partial y} & \dfrac{\partial^2}{\partial x\partial z} \end{bmatrix} \begin{bmatrix} \Pi_e \\ \Pi_h \end{bmatrix} \qquad (8b)$$

The variables' separation permits to write

$$\Pi_{e(h)}(x,y,z) = \Pi_{e(h)}(x).\Pi_{e(h)}(y).\Pi_{e(h)}(z) \qquad (9)$$

The developed fields in each region verify the following limit conditions:

$E_t = 0$ on a perfect electric conductor (10a)

$H_t = 0$ on a perfect magnetic conductor (10b)

The index t is for the tangential component.

For the interfaces Ω_j, where the metal is absent $(\Omega_j = \Omega_j^I)$, we apply the following continuity condition

$$E_T^{(j+1)}(d_j, y, z) = E_T^{(j)}(d_j, y, z) \qquad (11a)$$

$$H_T^{(j+1)}(d_j, y, z) - H_T^{(j)}(d_j, y, z) = 0 \qquad (11b)$$

T designate the tangential components of the electromagnetic field in the interface (yoz).

For the remaining interfaces Ω_l, where the metal is disposed $(\Omega_l = \Omega_l^M)$, we apply the following continuity

$$E_T^{(l+1)}(d_l, y, z) = E_T^{(l)}(d_l, y, z) \qquad (12)$$

The tangential components of the electric field and the electrical flow density of the surface are null on the metal and on the dielectric respectively

$$E_T^{(l)}(d_l, y, z) = 0 \quad \text{on} \quad \Omega_l^M \qquad (13a)$$

$$J_T^{(l)}(d_l, y, z) = 0 \quad \text{on} \quad \Omega_l^I \qquad (13b)$$

With

$$J_T^{(l)} = Z_0.u_n \times (H_T^{(l)} - H_T^{(l+1)}) \qquad (14)$$

u_n designates the unique director vector of the normal in the interfaces; $Z_0 = \sqrt{\dfrac{\mu_0}{\varepsilon_0}}$ is the impedance in the vacuum. It permits to make the implicated quantities homogenous in the equations (13a) and (13b). The conditions (13a) and (13b) can be written as follows

$$\delta_M E_T(\Omega_l^M) = 0 \qquad (15a)$$

$$\delta_I J_T(\Omega_l^I) = 0 \qquad (15b)$$

Where $\delta_M = \begin{cases} 1 & \text{on } \Omega_l^M \\ 0 & \text{on } \Omega_l^I \end{cases}$, and $\delta_I = 1 - \delta_M$.

δ_M and δ_I are the Heaviside indicators.

The continuity conditions are expressed like the following

$$\delta_M . E_T^l + \delta_I . J_T^l = 0 \quad \text{on } \Omega_l \tag{16}$$

The application of the LSBR method [7,10] consists on searching the minimum of the following functional

$$\begin{aligned} F(E_T^l, J_T^l) &= \delta_M < E_T^l / E_T^l > + \delta_I < J_T^l / J_T^l > \\ &= \delta_M . < E_y^l / E_y^l > + \delta_M . < E_z^l / E_z^l > \\ &\quad + \delta_I . < J_y^l / J_y^l > + \delta_I . < J_z^l / J_z^l > \end{aligned} \tag{17}$$

With

$$< E_y / E_y > H_M = \sum_{m,n=0}^{N} \int_{\Omega_l^M} E_y^{*t}(m) E_y(n) dy \tag{18a}$$

$$< J_y / J_y > H_I = \sum_{m,n=0}^{N} \int_{\Omega_l^I} J_y^{*t}(m) J_y(n) dy \tag{18b}$$

$m = 0, ..., N$; N is a natural integer. $n = 0, ..., N$

The trivial solution is not envisaged, we can define the norm $\mathcal{N}$ as a matrix which verifies the following condition

$$\left\langle E_T / \mathcal{N} / E_T \right\rangle = 1 \tag{19}$$

The truncation of the series permits to work in a space of finite dimensions. The series of development of the approached solution is better as the dimension of the space is large. The error brought about by the truncation is minimised by the least squares boundary residual method. We will have

$$\min \left\{ F(E_T^l, J_T^l) \right\} \tag{20}$$

It's a linear system of $(2N+1)$ equations.

The minimal eigenvalue $\lambda_{\min}$ [1] of the correspondent matrix of this system leads to the propagation constant k_z.

In the case of figures 2.a and 2.c where the planar structure under study is reduced on three regions disposed by the following fashion: dielectric1-ferrite-dielectric 3, in the guide with metal walls, we develop the Hertz potentials in functions series by using the following base which verifies the limits conditions

$$\Pi^e(x) = \begin{cases} (1): \sum_{n=0}^{+\infty} A_n^e . \cosh(k_{x.n}^{(1)} . x) \\ (2): \sum_{n=0}^{+\infty} B_n^e . \cosh(k_{x.n}^{(2)} . x) \\ \qquad + C_n^e . \sinh(k_{x.n}^{(2)} . x) \\ (3): \sum_{n=0}^{+\infty} D_n^e . \cosh(k_{x.n}^{(3)} . (h_3 - x)) \end{cases} \tag{21a}$$

$$\Pi^e(y) = \sqrt{\frac{2}{b}} . \sin(\alpha_n y) \tag{21b}$$

$$\Pi^e(z) = e^{-jk_z . z} \tag{21c}$$

$$\Pi^h(x) = \begin{cases} (1): \sum_{n=0}^{+\infty} A_n^h . \sinh(k_{x.n}^{(1)} . x) \\ (2): \sum_{n=0}^{+\infty} B_n^h . \sinh(k_{x.n}^{(2)} . x) \\ \qquad + C_n^h . \cosh(k_{x.n}^{(2)} . x) \\ (3): \sum_{n=0}^{+\infty} D_n^h . \sinh(k_{x.n}^{(3)} . (h_3 - x)) \end{cases} \tag{22a}$$

$$\Pi^h(y) = \sqrt{\frac{\sigma(n)}{b}} . \cos(\alpha_n y) \tag{22b}$$

$$\Pi^h(z) = e^{-jk_z . z} \tag{22c}$$

Where: $\alpha_n = \frac{n\pi}{b}$; $n \in IN$; $k_0 = \frac{\omega}{c}$;

$\mu_{r.2} = \mu_e = \frac{\mu^2 - \kappa^2}{\mu}$; $\sigma(n) = \begin{cases} 1 & \text{si } n = 0 \\ 2 & \text{si } n \neq 0 \end{cases}$

$$k_{x.n}^{(i)} = \left(\alpha_n^2 + k_z^2 - \varepsilon_{r.i}.\mu_{r.i}.k_0^2\right)^{1/2} \quad (23)$$

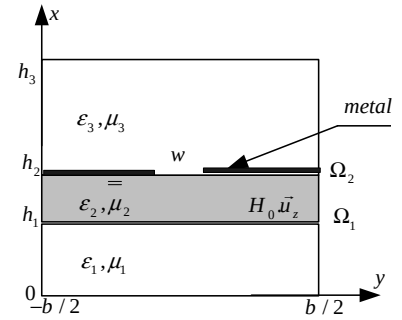

a)

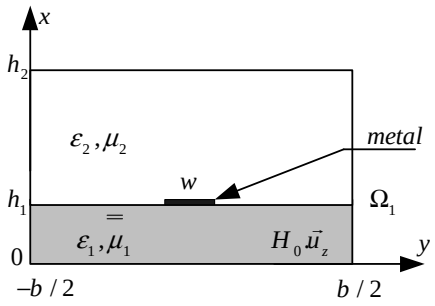

b)

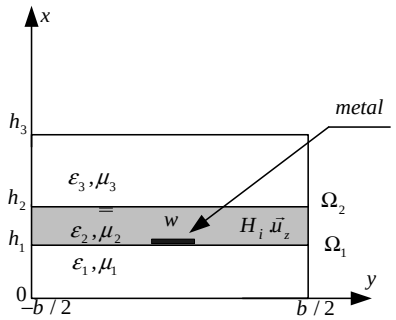

c)

Fig.2. a) Cross section of ferrite finlines. b) cross section of ferrite microstrip. c) The cross section of suspended ferrite microstrip

In the case of figure 2.b where the planar structure under study is reduced on two regions (microstrip line): ferrite-dielectric, in a guide with metal walls, we develop the Hertz potentials in functions series using the following base which verifies the limits conditions

$$\Pi^e(x) = \begin{cases} (1): \sum_{n=0}^{+\infty} A_n^e.\cosh(k_{x.n}^{(1)}.x) \\ (2): \sum_{n=0}^{+\infty} B_n^e.\cosh(k_{x.n}^{(2)}.(d_2 - x)) \end{cases} \quad (24)$$

$$\Pi^h(x) = \begin{cases} (1): \sum_{n=0}^{+\infty} A_n^h.\sinh(k_{x.n}^{(1)}.x) \\ (2): \sum_{n=0}^{+\infty} B_n^h.\sinh(k_{x.n}^{(2)}.(d_2 - x)) \end{cases} \quad (25)$$

Then, from the equations (7), (21) and (22), for the case of the figure 2.b for example, it is possible to develop each component of the field in a infinite series of dependant terms of integers n and coordinates x, y and z.

Because the use of the calculator needs to truncate to a finite number of terms, we suppose that the finite number of terms of the serie of index n is equal to N.

The number of unknown terms can be reduced to two by the application of six continuity conditions (11) and (12) in the interfaces Ω_1 and Ω_2. The conditions (13) are applied then in the interface Ω_2 and we obtain the following form of the electric field equations and the density of current

$$\begin{bmatrix} E_y \\ E_z \end{bmatrix} = \sum_{n=0}^{N} \left\{ A_n^e \begin{bmatrix} f_{11}(n) & 0 \\ 0 & f_{21}(n) \end{bmatrix} + A_n^h \begin{bmatrix} f_{12}(n) & 0 \\ 0 & f_{22}(n) \end{bmatrix} \right\} . \begin{bmatrix} \cos(\alpha_n y) \\ \sin(\alpha_n y) \end{bmatrix} \quad (26a)$$

$$\begin{bmatrix} J_y \\ J_z \end{bmatrix} = \sum_{n=0}^{N} \left\{ A_n^e \begin{bmatrix} g_{11}(n) & 0 \\ 0 & g_{21}(n) \end{bmatrix} + A_n^h \begin{bmatrix} g_{12}(n) & 0 \\ 0 & g_{22}(n) \end{bmatrix} \right\} \cdot \begin{bmatrix} \cos(\alpha_n y) \\ \sin(\alpha_n y) \end{bmatrix} \quad (26b)$$

By putting

$$\begin{bmatrix} \overline{A}_n^e \\ \overline{A}_n^h \end{bmatrix} = \begin{bmatrix} f_{11}(n) & f_{12}(n) \\ f_{21}(n) & f_{22}(n) \end{bmatrix} \cdot \begin{bmatrix} A_n^e \\ A_n^h \end{bmatrix}, \quad (27)$$

We have

$$\begin{bmatrix} E_y \\ E_z \end{bmatrix} = \sum_{n=0}^{N} \begin{bmatrix} \overline{A}_n^e & 0 \\ 0 & \overline{A}_n^h \end{bmatrix} \cdot \begin{bmatrix} \cos(\alpha_n y) \\ \sin(\alpha_n y) \end{bmatrix} \quad (28)$$

J_T will be exprimed as a function of $\overline{A}_n^e$ and $\overline{A}_n^h$ after the use of the following condition

$$\left\langle E_T / E_T \right\rangle = \sum_{n=0}^{N} \left| \overline{A}_n^e \right|^2 + \left| \overline{A}_n^h \right|^2 = 1, \quad (29)$$

We apply the LSBRM method, which takes into account the Gibbs phenomenon. This latter consists of generating an important error to the approached solution (which presents parasitic over-oscillations around the discontinuity points dielectric-metal) with respect to the exact solution

The components $E_T(y)$ and $J_T(y)$ present singularities [3,7], the development with trigonometric base functions rise the Gibbs phenomenon.

In the case of the microstrip line, of width b and of strip width w, the equalities (18a) and (18b) can be written as the following

$$< E_y / E_y > H_M = \sum_{m,n=0}^{N} \int_{-w/2}^{w/2} E_y^{*t}(m) E_y(n) dy \quad (30a)$$

$$< J_y / J_y > H_I = \sum_{m,n=0}^{N} \int_{-b/2}^{-w/2} J_y^{*t}(m) J_y(n) dy + \sum_{m,n=0}^{N} \int_{w/2}^{b/2} J_y^{*t}(m) J_y(n) dy \quad (30b)$$

To reduce the effect of the Gibbs phenomenon, we propose to modify the integration domain from the two sides (right and left) by a distance ε in the discontinuities of the metal-dielectric, like it is shown by figure 3, in order to avoid the over-oscillations region. Consequently, the equations (30a) and (30b) become

$$< E_y / E_y > H_M = \sum_{m,n=0}^{N} \int_{-w/2+\varepsilon}^{w/2-\varepsilon} E_y^{*t}(m) E_y(n) dy \quad (31a)$$

$$< J_y / J_y > H_I = \sum_{m,n=0}^{N} \int_{-b/2}^{-w/2-\varepsilon} J_y^{*t}(m) J_y(n) dy + \sum_{m,n=0}^{N} \int_{w/2+\varepsilon}^{b/2} J_y^{*t}(m) J_y(n) dy \quad (31b)$$

ε is defined [7] by $\varepsilon = \frac{b}{N}$, where N is the number of modes in the direction-oy.

We proceed by the same manner for the other components.

We define then the weight functions P_{1y} and P_{2y} (Fig. 3) as the following

$$P_{1y} = \begin{cases} 1 & si \ |y| < \left| \frac{w}{2} - \varepsilon \right| \\ 0 & si \ |y| > \left| \frac{w}{2} - \varepsilon \right| \end{cases} \quad (32a)$$

$$P_{2y} = \begin{cases} 1 & si \ |y| > \left| \frac{w}{2} + \varepsilon \right| \\ 0 & si \ |y| > \left| \frac{w}{2} + \varepsilon \right| \end{cases} \quad (32b)$$

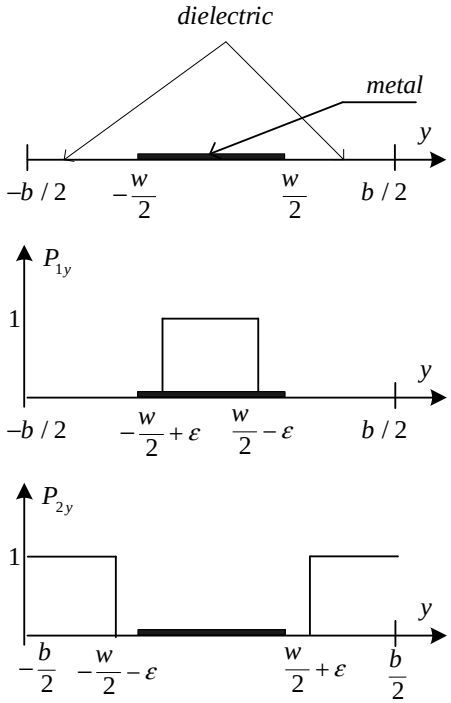

Fig.3. Weighting functions

In the general case, the continuity equations (15a) and (15b) become

$$P_{1y}(\Omega_l^M)E_T(\Omega_l^M)=0 \qquad (33a)$$

$$P_{2y}(\Omega_l^I)J_T(\Omega_l^I)=0 \qquad (33b)$$

The functional to minimise will be

$$F(E_T^l,J_T^l) = <E_T^l/P_1^+P_1/E_T^l> + <J_T^l/P_2^+P_2/J_T^l> \qquad (34)$$

The correspondent matrix is a square matrix of order $2.(N+1)$.

III. NUMERICAL RESULTS AND DISCUSSIONS

A. Finlines on a dielectric-ferrite substrate

The structure under study is formed by a finlines deposed on a dielectric-ferrite substrate like shown in the figure 2.a. The parameters of this structure are given by Table 1.

Table 1: The finlines parameters

h_1 (mm)	h_2 (mm)	h_3 (mm)	b (mm)	$4\pi M_S$ $(Gauss)$
3.302	3.556	7.112	3.556	2800

w/b	$\varepsilon_{r1}=\varepsilon_{r3}$	$\mu_{r1}=\mu_{r3}$	ε_{r2}
0.13	1	1	2.22

Figure 4 compares, at the frequency 26 GHz, the performances of the LSBR method and the LSBRM method by calculating the relative normalised propagation constant of the finlines structure shown in Figure 2.a the parameters of which are presented in Table 1.

The convergence of the solution is accelerated for the new variant of the LSBR method. This acceleration is shown on Figure 5 where we have plotted the curves of the normalised propagation constant k_Z/k_0 at the frequency 26 GHz with respect to the number of harmonics N. So, we can notice that with the LSBRM method, the curve decreases to be stabilised from the value N=8 and it is still close to the reference value. However, with the LSBR method, the curve is stabilised from the value N=12, but it's further from the reference value than the one made by the modified method.

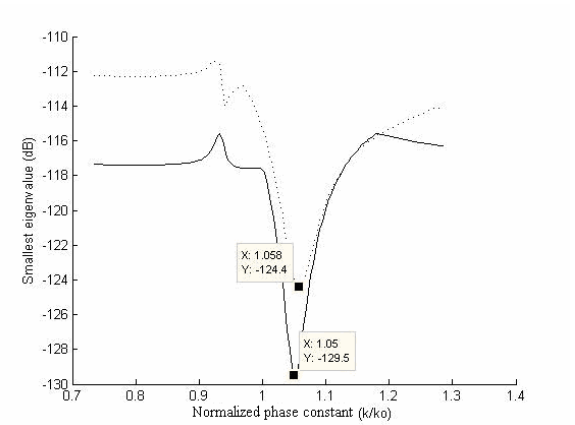

Fig.4. Performance comparison for M=0
_____ : LSBRM method
……. : LSBR method

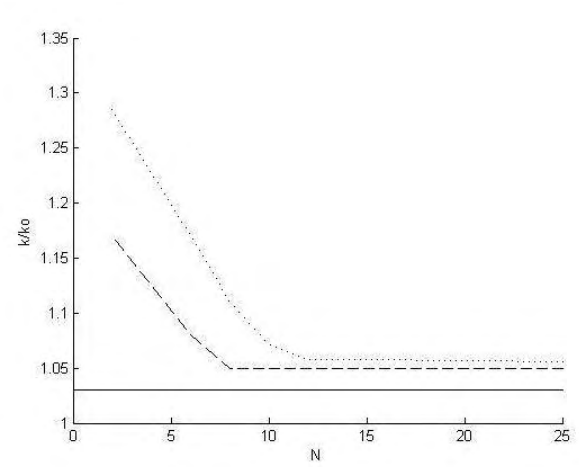

Fig.5. Normalized propagation constant as a function of the harmonics number N, with a frequency of 26 *GHz* .
_____ : experimental value of J. B. Knorr.
_ _ _ _ _ : our value with the LSBRM method.
…….. : our value with the LSBR method.

By applying the method of LSBR, we search, for a still frequency, the smallest eigenvalue with respect to the normalised propagation constant of the finlines, as shown by the figure 4.

If $M = 0$, then $\kappa = 0$ and $\mu = 1$. The permeability tensor of the ferrite become scalar and it is equal to $\mu_{r2} = 1$. The ferrite becomes, in this case, an isotropic dielectric.

For the non magnetized ferrite $(M = 0)$ and for the frequency $f = 26\,GHz$, the minimal eigenvalue is obtained at -129,5 dB, which corresponds to $k_z/k_0 = 1{,}05$ (fig. 4).

By varying the frequency, we obtain the dispersion curve for different values of M when $M < M_S$ and M_S is the saturation magnetization.

The simulations results for $M = 0$ are in very good agreement (with a difference of 1 to 2 %) with the empirical results of J. B. Knorr [11].

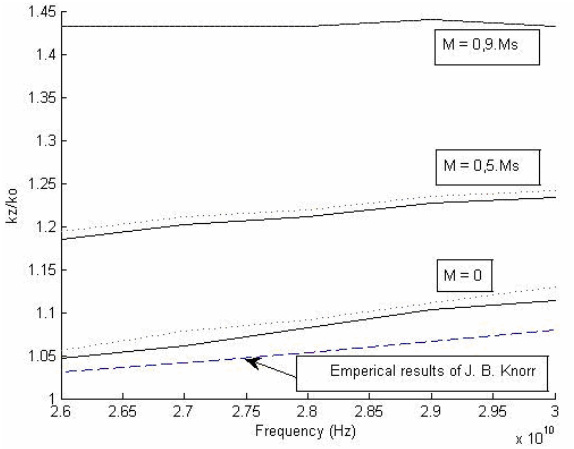

Fig.6. The dispersion curves of the finlines for different values of the magnetization M.
_ _ _ _ _ : [11] emperical results of J. B. Knorr
…….. : The LSBR method
_____ : The LSBRM method

If *M* increases, the values of the normalised propagation constant increase (fig. 6). This variation is confirmed by the results of the reference [12]. This permits to confirm the efficiency of the developed numeric model.

B. Microstrip line on a ferrite substrate

Table 2 : The microstrip parameters

h_1 (mm)	h_2 (mm)	b (mm)	$4\pi M_S$ $(Gauss)$
1.27	12.70	12.70	2800

w/b	$\varepsilon_{r1} = \varepsilon_{rf}$	μ_{r2}	ε_{r2}
0.10	8.875	1	1

The analysis of the structure, formed by a simple microstrip line deposed on a ferrite substrate (fig. 2.b) which the parameters are given by table 2, permits to calculate the normalised propagation constant in the frequency band [12 – 15] GHz.

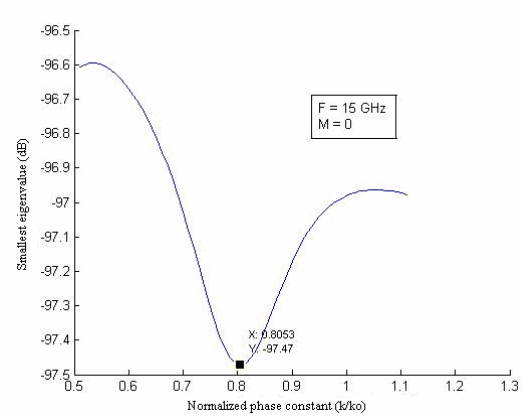

Fig.7. Variation of the minimal eigenvalue (dB) as a function of k_z / k_0 for the structure of the figure 2.b with $M = 0$

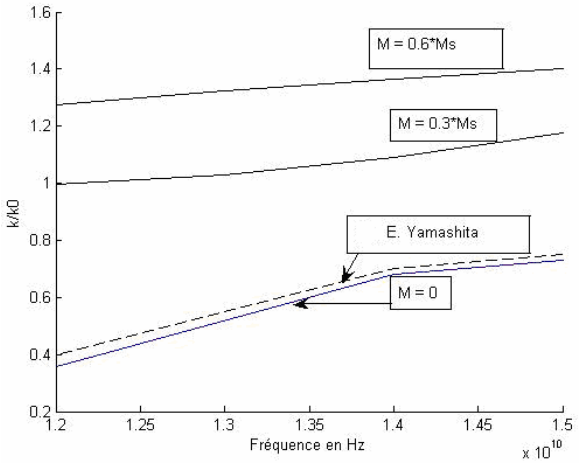

Fig.8. The dispersion curves of the microstrip for different values of the magnetization M

_ _ _ _ _ : Integral equation method of [13]

_____ : our results with the LSBRM method.

When the ferrite is not magnetized, the curve (fig. 8) shows a good coherence with the simulated results of E. Yamashita [13] who use an integral equation method based on a discretization of the integration domain. The error in the high first order mode is smaller than 3 %. The used number of harmonics is N=15. Besides, the propagation constant increases when the ferrite magnetization increases.

C. Microstrip line on a dielectric - ferrite substrate

The structure under study is formed by a simple microstrip deposed on a dielectric-ferrite substrate as it is shown in figure 2.c. The parameters of this structure are given by Table 3.

Table 3: The microstrip parameters

h_1 (mm)	h_2 (mm)	h_3 (mm)	b (mm)	w (mm)
1	0.5	4	11	1

$\varepsilon_{r1} = \varepsilon_{r2}$	$\mu_{r1} = \mu_{r3}$	ε_{r3}	$4\pi M_S$ $(Gauss)$
10	1	1	1800

The analysis of the structure permits to calculate the normalised propagation constant in the frequency band [4 – 11] GHz.

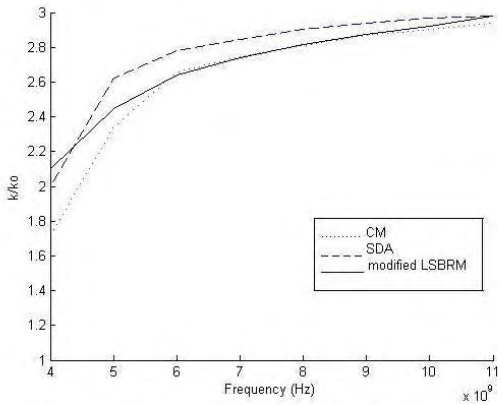

Fig.9. Dispersion diagrams of the single ferrite microstrip (FSL), shown in fig.2.c ($H_0 = 0\ kA/m$)

_ _ _ _ _ : SDA method [14]

.....: Coupled-Mode method [14]

_____ : our results with the LSBRM method.

The simulation results (fig. 9) for $H_0 = 0$ are in very good agreement with the results of J. Mazur [14]. This permits to confirm the efficiency of the developed numerical model.

IV. CONCLUSION

In this paper, we have presented a new variant of the LSBR method based on the consideration of field singularity in the metal-dielectric

discontinuities due to the existence of the Gibbs phenomenon. This method systematically necessitates weight functions and it is applied to the study of the propagation constant of some planar structures.

A direct extension of this technique has been developed to take into account anisotropic materials like ferrites.

The LSBRM method brings an appreciated improvement with respect to the LSBR method. It is mostly characterized by a clearly better minimum of eigenvalues and a high speed convergence. The so obtained results match perfectly those published in the literature.

The variation of the trajectory of the dispersion as a function of M shows the importance of the planar circuits [15] as it is the case for these phase-converters with a magnetic command.

ACKNOWLEDGEMENTS

The author would like to thank the anonymous reviewers for their insightful remarks and helpful suggestions.

REFERENCES

[1] H. Baudrand, M. Boussouis and J. L. Amalric, "Analysis of some planair structures by the least-squares boundary residual method", ***IEEE Trans. Microwave Theory Tech***., Vol. MTT-34, No. 2, pp. 298-301, Feb. 1986.

[2] R. Mittra and T. Itoh, "A new technique for the analysis of dispersion characteristics of microstrip lines", ***IEEE Trans. Microwave Theory Tech.***, Vol. MTT-19, pp. 47-56, Jan. 1971.

[3] C. J. Railton and T. Rozzi, "Complex Modes in Boxed Microstrip", ***IEEE Trans MTT***, Vol 36, No. 5, pp 865-874, May 1988.

[4] T. Itoh and R. Mittra, "Spectral domain approach for calculating the dispersion characteristics of microstrip lines", ***IEEE Trans. Microwave Theory Tech***., Vol. MTT-21, pp. 496-499, Jul. 1973.

[5] M. Mazur, E. Sedek and J. Mazur, "Propagation in a ferrite circular waveguide magnetized through a rotary four-pole magnetic field", ***Progress In Electromagnetics Research, PIER*** 68, 1–13, 2007.

[6] R M. Matsunaga, "A coupled-mode theory-based analysis of coupled microstrip lines on a ferrite substrate", ***Progress In Electromagnetics Research, PIER*** 42, 219–232, 2003.

[7] M. L. Riabi, M. Ahmadpanah, H. Benzina, H. Baudrand and V. Fouad Hanna, "Performance of the LSBRM using efficient weighting functions for planar structures", ***IEE Proc,-Microw. Antennas Propag***, Vol. 142, No. 4, pp. 364-368, August 1995.

[8] J. J. Green and F. Sandy, "Microwave characterization of partially magnetized ferrites", ***IEEE-trans, Vol. MTT***-22, pp. 641-645, Jaune 1974.

[9] E. Schloemann, "Microwave behavior of partially magnetized ferrites", ***J. Appl. Phys***., Vol. 1, p. 1204, June 1970.

[10] S. Bolioli, H. Benzina, H. Baudrand, and B. Chan, "Centimeter-wave microstrip phase shifter on a ferrite-dielectric substrate", ***IEEE Trans***., MTT-37, No. 4, pp. 698-705, April 1989.

[11] J. B. Knorr and P. M. Shayda, "Millimeter-wave finline characteristics", ***IEEE trans. MTT***, Vol. 28, No. 7, pp. 737-743, Jul. 1980.

[12] Y. C. Moon, J. R. Lee, S. W. Yun and I. S. Chang, "A broadband planar isolator using coupled microstrip lines on a magnetized gyrotropic substrate", ***Microwave Journal***, Vol. 44, No. 11, November 2001.

[13] E. Yamashita, "Analysis of microstrip-like transmission lines by nonuniform discretization of integral equations", ***IEEE trans MTT***, Vol. 24, No. 4, pp. 195-200, Apr. 1976.

[14] J. Mazur, P. Kutysz, and A. Cwikla, "Coupled-mode analysis of ferrite microstrip lines", ***IEEE Microwave Guided Wave Lett***., Vol. 9, pp. 300–302, Aug. 1999.

[15] H. Sakli, H. Benzina, T. Aguili and J. W. Tao, "A rigorous study of complex modes by applying the transverse operator in a rectangular guide of ferrites", *International Journal of Microwave and Optical Technology*, *IJMOT*, Vol. 3, No. 5, pp. 535-540, Nov. 2008.